Inorganic Chemistry
Article

Inorg. Chem. **2010**, *49*, 73–81 **73**
DOI: 10.1021/ic901374f

Reaction of a (Salen)ruthenium(VI) Nitrido Complex with Thiols. C−H Bond Activation by (Salen)ruthenium(IV) Sulfilamido Species

Wai-Lun Man,[†] William W. Y. Lam,[†] Hoi-Ki Kwong,[†] Shie-Ming Peng,[‡] Wing-Tak Wong,[§] and Tai-Chu Lau*,[†]

[†]*Department of Biology and Chemistry, City University of Hong Kong, Tat Chee Avenue, Kowloon Tong, Hong Kong, China,* [‡]*Department of Chemistry, National Taiwan University, Taipei 106, Taiwan, and* [§]*Department of Chemistry, The University of Hong Kong, Pokfulam Road, Hong Kong, China*

Received July 14, 2009

The reaction of $[Ru^{VI}(N)(L)(MeOH)](PF_6)$ [**1**; L = *N*,*N*′-bis(salicylidene)-*o*-cyclohexyldiamine dianion] with a stoichiometric amount of RSH in CH_3CN gives the corresponding (salen)ruthenium(IV) sulfilamido species $[Ru^{IV}\{N(H)SR\}(L)(NCCH_3)](PF_6)$ (**2a**, R = ^{t}Bu; **2b**, R = Ph). Metathesis of **2a** with NaN_3 in methanol affords $[Ru^{IV}\{N(H)S^tBu\}(L)(N_3)]$ (**2c**). **2a** undergoes further reaction with 1 equiv of RSH to afford a (salen)ruthenium(III) sulfilamine species, $[Ru^{III}\{N(H)_2S^tBu\}(L)(NCCH_3)](PF_6)$ (**3**). On the other hand, **2b** reacts with 2 equiv of PhSH to give a (salen)ruthenium(III) ammine species $[Ru^{III}(NH_3)(L)(NCCH_3)](PF_6)$ (**4**); this species can also be prepared by treatment of **1** with 3 equiv of PhSH. The X-ray structures of **2c** and **4** have been determined. Kinetic studies of the reaction of **1** with excess RSH indicate the following schemes: **1** → **2a** → **3** (R = ^{t}Bu), **1** → **2b** → **4** (R = Ph). The conversion of **1** to **2** probably involves nucleophilic attack of RSH at the nitrido ligand, followed by a proton shift. The conversions of **2a** to **3** and **2b** to **4** are proposed to involve rate-limiting H-atom abstraction from RSH by **2a** or **2b**. **2a** and **2b** are also able to abstract H atoms from hydrocarbons with weak C−H bonds. These reactions occur with large deuterium isotope effects; the kinetic isotope effect values for the oxidation of 9,10-dihydroanthracene, 1,4-cyclohexadiene, and fluorene by **2a** are 51, 56, and 11, respectively.

Introduction

Osmium(VI) nitrido complexes containing nitrogen-based ligands such as *cis*- or *trans*-$[Os^{VI}(N)(tpy)Cl_2]^+$ (tpy = 2,2′:6′,2″-terpyridine), $[Os^{VI}(N)(tpm)Cl_2]^+$ [tpm = tris(1-pyrazolyl)methane], $[Os^{VI}(N)(Tp)Cl_2]$ [Tp = hydrotris(1-pyrazolyl)-borate], and $[Os^{VI}(N)(bpy)Cl_3]$ (bpy = 2,2′-bipyridine) have been shown to exhibit novel electrophilic properties.[1−3] The reaction of *trans*- or *cis*-$[Os^{VI}(N)(tpy)Cl_2]^+$ with thiols produces the corresponding osmium(IV) sulfilimido species, *trans*- or *cis*-$[Os^{IV}\{NS(H)R\}(tpy)Cl_2]^+$ (R = Ph, 4-MePh, or 3,5-Me_2-Ph). These osmium(IV) sulfilimido species undergo a number of novel redox reactions, including proton-coupled electron transfer (PCET)[4] and proton-induced reversible uptake of O_2.[5] The corresponding sulfoximido species also undergo novel O-atom-transfer reactions.[6,7]

We recently reported a highly electrophilic (salen)ruthenium(VI) nitrido species, $[Ru^{VI}(N)(L)(MeOH)](PF_6)$ [**1**; L = *N*,*N*′-bis(salicylidene)-*o*-cyclohexyldiamine dianion], that reacts readily with secondary amines, alkenes, or isocyanides to form ruthenium(IV) hydrazido(1−), ruthenium(III) aziridine, and ruthenium(III) carbodiimido complexes, respectively.[8−10] We report herein that **1** undergoes rapid stepwise reactions with thiols to produce ruthenium(IV) sulfilamido, ruthenium(III) sulfilamine, and ruthenium(III) ammine species. The (salen)ruthenium(IV) sulfilamido species are also able to abstract H atoms from hydrocarbons with weak C−H bonds. The structure of the salen ligand used in this work is shown in Figure 1.

*To whom correspondence should be addressed. E-mail: bhtclau@cityu.edu.hk.

(1) Huynh, M. H. V.; Meyer, T. J. *Inorg. Chem.* **2003**, *42*, 8140−8160 and references cited therein.
(2) (a) Dehestani, A.; Kaminsky, W.; Mayer, J. M. *Inorg. Chem.* **2003**, *42*, 605–611. (b) Crevier, T. J.; Mayer, J. M. *J. Am. Chem. Soc.* **1998**, *120*, 5595–5596. (c) McCarthy, M. R.; Crevier, T. J.; Bennett, B.; Dehestani, A.; Mayer, J. M. *J. Am. Chem. Soc.* **2000**, *122*, 12391–12392. (d) Crevier, T. J.; Lovell, S.; Mayer, J. M. *J. Am. Chem. Soc.* **1998**, *120*, 6607–6608.
(3) (a) Brown, S. N. *J. Am. Chem. Soc.* **1999**, *121*, 9752–9753. (b) Brown, S. N. *Inorg. Chem.* **2000**, *39*, 378–381. (c) Maestri, A. G.; Cherry, K. S.; Toboni, J. J.; Brown, S. N. *J. Am. Chem. Soc.* **2001**, *123*, 7459–7460.
(4) Huynh, M. H. V.; White, P. S.; Meyer, T. J. *Angew. Chem., Int. Ed.* **2000**, *39*, 4101–4104.
(5) Huynh, M. H. V.; Morris, D. E.; White, P. S.; Meyer, T. J. *Angew. Chem., Int. Ed.* **2002**, *41*, 2330–2333.
(6) Huynh, M. H. V.; White, P. S.; Meyer, T. J. *J. Am. Chem. Soc.* **2001**, *123*, 9170–9171.
(7) Huynh, M. H. V.; Baker, R. T.; Morris, D. E.; White, P. S.; Meyer, T. J. *Angew. Chem., Int. Ed.* **2002**, *41*, 3870–3873.
(8) Man, W. L.; Tang, T. M.; Wong, T. W.; Lau, T. C; Peng, S. M.; Wong, W. T. *J. Am. Chem. Soc.* **2004**, *126*, 478–479.
(9) Man, W. L.; Lam, W. W. Y.; Yiu, S. M.; Lau, T. C.; Peng, S. M. *J. Am. Chem. Soc.* **2004**, *126*, 15336–15337.
(10) Kwong, H. K.; Man, W. L.; Xiang, J.; Wong, W. T.; Lau, T. C. *Inorg. Chem.* **2009**, *48*, 3080–3086.

Published on Web 12/02/2009

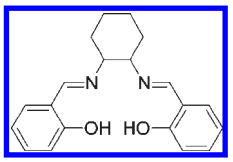

Figure 1. Structure of H_2L.

Experimental Section

Materials. The complex $[Ru^{VI}(N)(L)(MeOH)](PF_6)$ (**1**) was prepared by a literature method.[8] The Schiff base ligand H_2L [L = *N*,*N*′-bis(salicylidene)-*o*-cyclohexylenediamine dianion] was synthesized by condensation of salicylaldehyde with *trans*-1,2-cyclohexyldiamine in refluxing ethanol. Thiols (Aldrich) were freshly distilled over anhydrous $CaCl_2$ before use. ^{t}BuSD and PhSD (>95% D by ^{1}H NMR) were prepared by the direct deuterium exchange of ^{t}BuSH and PhSH with 99.8% D_2O (ARMAR AG), and the processes were repeated three times.[11] 9,10-Dihydroanthracene (DHA; Aldrich, 97%), xanthene (Aldrich, 99%), fluorene (Aldrich, 98%), diphenylmethane (Aldrich, 99%), and triphenylmethane (Aldrich, 99%) were recrystallized twice from ethanol. 1,4-Cyclohexadiene (CHD) was dried over CaH_2 and then distilled under dinitrogen. DHA-d_4 and CHD-d_8 [both >99% D by ^{1}H NMR and gas chromatography−mass spectrometry (GC−MS)] were prepared by a literature method.[12] ^{n}Bu$_4$NPF$_6$ (Aldrich) for electrochemistry was recrystallized three times from boiling ethanol and dried in vacuo at 120 °C for 24 h. Acetonitrile (Aldrich) for electrochemistry was distilled over calcium hydride. All other chemicals were of reagent grade and were used without further purification.

Instrumentation. IR spectra were recorded as KBr pellets on a Nicolet Avatar 360 FT-IR spectrophotometer at 4 cm^{-1} resolution. Elemental analyses were done on an Elementar Vario EL analyzer. ^{1}H NMR spectra were recorded on a Bruker (400 MHz) FT-NMR spectrometer. The chemical shifts (δ, ppm) were reported with reference to tetramethylsilane. UV/vis spectra were recorded with a Perkin-Elmer Lamda 19 spectrophotometer in 1 cm quartz cuvettes. Magnetic measurement (solid sample, Gouy method) was performed at 20 °C using a Sherwood magnetic balance (Mark II). Electrospray ionization mass spectrometry (ESI/MS) spectra were obtained on a PE SCIEX API 365 mass spectrometer. The analyte solution was continuously infused with a syringe pump at a constant flow rate of 5 μL min^{-1} into the pneumatically assisted electrospray probe, with nitrogen as the nebulizing gas. The declustering potential was typically set at 10−20 V. Cyclic voltammetry (CV) was performed with a PAR model 273 potentiostat using a glassy carbon working electrode, a $Ag/AgNO_3$ (0.1 M in CH_3CN) reference electrode, and a Pt wire counter electrode with ferrocene (Cp_2Fe) as the internal standard. GC analyses were performed on a HP 7890 GC/FID equipped with a HP-5MS (30 m × 0.25 mm i.d.) column. GC−MS measurements were carried out on a HP 6890 gas chromatograph interfaced to a HP 5975 mass-selective detector.

Preparations. **$[Ru^{IV}\{N(H)S^tBu\}(L)(NCCH_3)](PF_6)$ (2a).** ^{t}BuSH (9 mg, 0.1 mmol) was slowly added with stirring to an orange solution of **1** (61 mg, 0.1 mmol) in CH_3CN (3 mL) at room temperature. After 15 min, Et_2O (30 mL) was carefully layered onto the deep-blue solution, and the mixture was allowed to stand for 3 h at 0 °C. The resulting dark-blue microcrystalline solid was filtered and recrystallized by the slow diffusion of Et_2O into a solution of the complex in CH_3CN at room temperature. Yield: 56%. ^{1}H NMR (400 MHz, DMSO-d_6): δ 16.41 (s, 1H, NH), 8.63 (s, 1H, N=CH), 8.51 (s, 1H, N=CH), 7.57 (d, J = 8.0 Hz, 2H), 7.41 (t, J = 8.0 Hz, 2H), 7.31−7.39 (m, 2H), 6.70 (t, J = 7.6 Hz, 2H), 4.59−4.64 (m, 1H, N−CH), 3.96−4.02 (m, 1H, N−CH), 3.08−3.18 (m, 2H), 2.08−2.13 (m, 2H), 2.06 (s, 3H, $NCCH_3$), 1.81−1.86 (m, 2H), 1.59−1.67 (m, 2H), 0.98 (s, 9H, CH_3 on ^{t}Bu). IR (KBr, cm^{-1}): ν(N−H) 3236(s), ν(C≡N) 2321, 2292(w), ν(C=N) 1603(s), ν(P−F) 847(s). Anal. Calcd (found) for $C_{26}H_{33}N_4O_2SPF_6Ru$: C, 43.88 (43.67); H, 4.67 (4.76); N, 7.87 (8.00). UV/vis (CH_3CN): λ_{max} [nm] (ε [mol^{-1} dm^3 cm^{-1}]): 597 (3780), 390 (9230), 335 (13 000), 228 (36 400). ESI/MS in CH_3CN: m/z 567 (M^+), 526 ($M^+ - CH_3CN$).

$[Ru^{IV}\{N(H)SPh\}(L)(NCCH_3)](PF_6)$ (2b). The blue solid was prepared by a procedure similar to that for **2a** using benzenethiol. Yield: 70%. ^{1}H NMR (400 MHz, DMSO-d_6): δ 16.69 (s, 1H, NH), 8.65 (s, 1H, N=CH), 8.59 (s, 1H, N=CH), 7.66 (d, J = 7.4 Hz, 1H, *o*-CH on PhS), 7.61 (d, J = 7.4 Hz, 1H, *o*-CH on PhS), 7.45−7.53 (m, 3H, one *p*-CH on PhS and two CH on L), 7.36−7.42 (m, 2H), 7.29 (t, J = 7.7 Hz, 2H), 6.91−6.95 (m, 2H, *m*-CH on PhS), 6.74−6.81 (m, 2H), 4.50−4.55 (m, 1H, N−CH), 4.01−4.06 (m, 1H, N−CH), 3.11−3.19 (m, 2H), 2.08−2.14 (m, 2H), 2.06 (s, 3H, $NCCH_3$), 1.82−1.97 (m, 2H), 1.52−1.63 (m, 2H). IR (KBr, cm^{-1}): ν(N−H) 3244(s), ν(C≡N) 2313, 2286(w), ν(C=N) 1601(s), ν(P−F) 839(s). Anal. Calcd (found) for $C_{28}H_{29}N_4O_2SPF_6Ru$: C, 45.97 (46.18); H, 3.99 (4.11); N, 7.66 (7.88). UV/vis (CH_3CN): λ_{max} [nm] (ε [mol^{-1} dm^3 cm^{-1}]): 616 (5030), 398 (9240), 335 (13 900), 220 (41 200). ESI/MS in CH_3CN: m/z 587 (M^+), 546 ($M^+ - CH_3CN$).

$[Ru^{IV}\{N(H)S^tBu\}(L)(N_3)]\cdot CH_3OH$ (2c). This was prepared by metathesis of **2a** (100 mg, 0.14 mmol) with NaN_3 (10 mg, 0.15 mmol) in methanol (10 mL). The solution slowly deposited dark-red single crystals suitable for X-ray crystallography. Yield: (80%). IR (KBr, cm^{-1}): ν(N−H) 3076(s), ν(N_3) 2034(s). Anal. Calcd (found) for $C_{24}H_{30}N_6O_2SRu\cdot CH_3OH$: C, 50.07 (50.15); H, 5.71 (5.49); N, 14.01 (14.27). UV/vis (CH_3CN): λ_{max} [nm] (ε [mol^{-1} dm^3 cm^{-1}]): 467 (7400), 378 (10 000), 335 (8300), 227 (36 900).

$[Ru^{III}\{N(H)_2S^tBu\}(L)(NCCH_3)](PF_6)\cdot 0.5CH_3CN$ (3). PhSH (11 mg, 0.10 mmol) was added to a blue solution of **2a** (70 mg, 0.10 mmol) in CH_3CN (10 mL), and the mixture was stirred for 3 h at room temperature under argon. The green solution was then concentrated to ca. 1 mL; the addition of Et_2O (20 mL) precipitated a green solid, which was collected and washed with Et_2O. Yield: 90%. IR (KBr, cm^{-1}): ν(N−H) 3289(w), 3133(w), ν(C≡N) 2322(w), 2293(w), 2250(w), ν(P−F) 841(s). Anal. Calcd (found) for $C_{26}H_{34}N_4O_2SPF_6Ru\cdot 0.5CH_3CN$: C, 44.23 (44.22); H, 4.88 (4.62); N, 8.60 (8.45). UV/vis (CH_3CN): λ_{max} [nm] (ε [mol^{-1} dm^3 cm^{-1}]) 686 (3630), 479 (2490), 347 (13 700), 230 (37 900), 216 (34 600). ESI/MS in CH_3CN: m/z 568 (M^+), 527 ($M^+ - CH_3CN$). Magnetic measurement: μ_{eff} = 1.98 μ_B.

$[Ru^{III}(NH_3)(L)(NCCH_3)](PF_6)\cdot CH_3CN$ (4). PhSH (53 mg, 0.48 mmol) was added with stirring to an orange solution of **1** (100 mg, 0.16 mmol) in CH_3CN (20 mL) at room temperature. Slow evaporation of the green solution afforded dark-green single crystals suitable for X-ray crystallography after 2 days. Yield: 67%. IR (KBr, cm^{-1}): ν(N−H) 3341(s), 3237(w), 3135(s), ν(C≡N) 2323(w), 2292(w), 2250(w), ν(P−F) 837(s). Anal. Calcd (found) for $C_{22}H_{26}N_4O_2PF_6Ru\cdot CH_3CN$: C, 43.31 (43.52); H, 4.39 (4.59); N, 10.52 (10.46). UV/vis (CH_3CN): λ_{max} [nm] (ε [mol^{-1} dm^3 cm^{-1}]) 680 (4500), 492 (1800), 349 (14 600), 232 (34 400), 216 (34 600). ESI/MS in CH_3CN: m/z 480 (M^+). Magnetic measurement: μ_{eff} = 2.04 μ_B.

Kinetics. The kinetics of the reactions were studied under argon by using either a Hewlett-Packard 8452 diode-array spectrophotometer, a Perkin-Elmer Lambda 19 UV/vis/near-IR spectrophotometer, or a Hi-Tech Scientific SF-61 stopped-flow spectrophotometer (path length = 1 cm). The concentrations of the substrates were at least in 10-fold excess of that of the ruthenium complexes. Pseudo-first-order rate constants, k_{obs}, were obtained by nonlinear least-squares fits of A_t vs time t according to the equation $A_t = A_\infty + (A_0 - A_\infty)\exp(-k_{obs}t)$, where A_0 and A_∞ are the initial and final absorbances,

(11) Earnshaw, D. G.; Cook, G. L.; Dinneen, G. U. *J. Phys. Chem.* **1964**, *68*, 296–300.
(12) Goldsmith, C. R.; Jonas, R. T.; Stack, T. D. P. *J. Am. Chem. Soc.* **2002**, *124*, 83–96.

Table 1. Crystal Data and Structure Refinement Details for Compounds **2c** and **4**

	2c	**4**
formula	$C_{25}H_{34}N_6O_3RuS$	$C_{24}H_{29}F_6N_5O_2PRu$
M_r	599.71	665.56
cryst dimens/mm	0.34 × 0.26 × 0.17	0.22 × 0.20 × 0.20
cryst syst	triclinic	triclinic
space group	$P\bar{1}$	$P\bar{1}$
a/Å	8.017(1)	10.2410(6)
b/Å	13.099(2)	10.2840(6)
c/Å	14.887(2)	13.1374(7)
α/deg	105.71(1)	92.783(1)
β/deg	100.37(1)	90.788(1)
γ/deg	92.53(1)	104.8580(1)
V/Å^3	1473.2(4)	1335.28(13)
Z	2	2
ρ_{calcd}/Mg m^{-3}	1.352	1.655
F(000)	620	674
no. of reflns collcd	6378	6111
no. of obsd reflns [$I > 2\sigma(I)$]	5000	5758
final R indices, $I > 2\sigma(I)$	R1 = 0.0460, wR2 = 0.0590	R1 = 0.0496, wR2 = 0.1284
GOF	1.016	1.181
no. of param	361	363

respectively. Activation parameters were obtained from the plot of $\ln(k_2/T)$ vs $1/T$ according to the Eyring equation.

Analysis of Organic Products. Products of the reaction of hydrocarbons were analyzed by GC and GC−MS. Disulfides were analyzed by the following method. The filtrate after the reaction was loaded onto a short column of silica gel (1 × 3 cm) and eluted with Et_2O. Removal of the volatiles under vacuum gave air-stable disulfide as a white solid, which was characterized by ^{1}H NMR and GC−MS.

X-ray Crystallography. Measurements of **2c** and **4** were collected on a Bruker SMART 1000 CCD area-detector diffractometer using graphite-monochromated Mo Kα radiation (λ = 0.710 73 Å) at 293 K. Details of the intensity data collection and crystal data are given in Table 1. The raw intensity data frames were integrated with the *SAINT+* program using a narrow-frame integration algorithm.[13] Corrections for Lorentz and polarization effects were also applied by *SAINT*. For each analysis, an empirical absorption correction based on multiple measurements of equivalent reflections was applied by using the program *SADABS*.[14] The structures were solved by direct methods and expanded by difference Fourier syntheses using the software *SHELTXL*.[15] Structure refinements were made on F^2 by the full-matrix least-squares technique. The non-H atoms were refined with anisotropic displacement parameters. The H atoms were placed in their ideal positions but not refined.

Results and Discussion

Reaction of 1 with 1 equiv of RSH: Formation of (Salen)ruthenium(IV) Sulfilamido Species 2a−2c. The treatment of **1** with 1 equiv of RSH in CH_3CN produced dark-blue $[Ru^{IV}\{N(H)SR\}(L)(NCCH_3)]PF_6$ (**2a**, R = ^{t}Bu; **2b**, R = Ph) (eq 1).

$$[Ru^{VI}(N)(L)(NCCH_3)]^+ + RSH \rightarrow [Ru^{IV}\{N(H)SR\}(L)(NCCH_3)]^+ \quad (1)$$

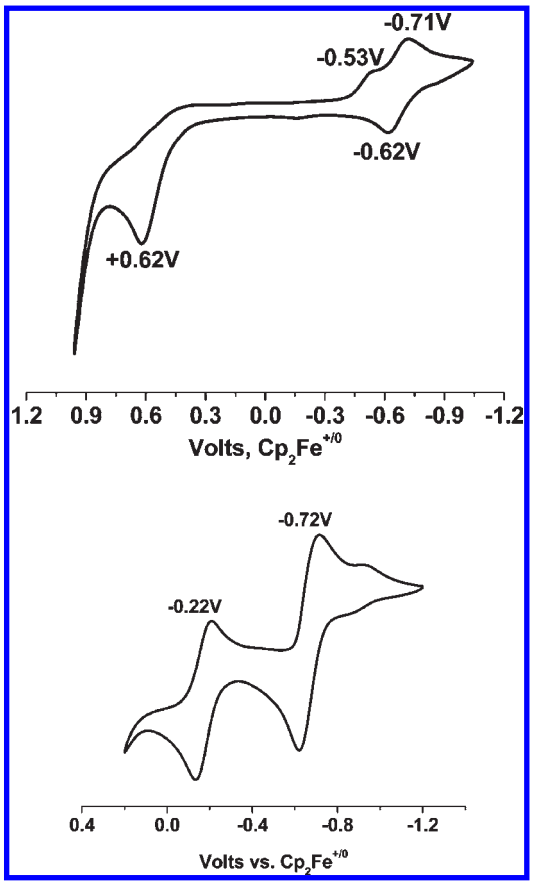

Figure 2. Cyclic voltammograms of **2a** (top) and after the addition of Et_3N (bottom) in CH_3CN.

Compounds **2a** and **2b** are diamagnetic (solid sample, Gouy method), similar to the reported ruthenium(IV) hydrazido(1−) species, $[Ru^{IV}\{N(H)NC_4H_8\}(L)\{N(H)C_4H_8\}]^+$.[8] In the ^{1}H NMR spectra in $(CD_3)_2SO$, the two imine protons occur as two singlets at δ 8.51 and 8.63 for **2a** and at δ 8.59 and 8.65 for **2b** (Figure S1 in the Supporting Information). The methyl protons of the ^{t}BuSNH moiety in **2a** occur as a singlet at δ 0.98. The broad resonances at δ 16.41 in **2a** and δ 16.69 for **2b** are assigned to N−H of the sulfilamido ligands; these peaks disappear upon the addition of D_2O (5% by volume). The existence of N−H in **2a** and **2b** is also evidenced from their IR spectra, which show a sharp band at 3236 cm^{-1} for **2a** and at 3244 cm^{-1} for **2b**. ESI/MS of **2a** (Figure S2 in the Supporting Information) shows peaks at m/z 567 ($[M]^+$) and 526 ($[M - CH_3CN]^+$); similarly, ESI/MS of **2b** shows peaks at m/z 587 ($[M]^+$) and 546 ($[M - CH_3CN]^+$).

The cyclic voltammogram of **2a** in CH_3CN (Figure 2) displays an irreversible oxidation wave at E_{pa} = +0.62 V, an irreversible reduction wave at E_{pc} = −0.53 V, and a reversible reduction wave centered at −0.67 V (vs $Cp_2Fe^{+/0}$). Because the reversible reduction wave occurs at the same potential as that of **3** (see below), it is assigned to the $[Ru^{III}\{N(H)_2S^tBu\}(L)(NCCH_3)]^+/[Ru^{II}\{N(H)_2S^tBu\}(L)(NCCH_3)]$ couple. The irreversible wave at −0.53 V is probably due to the PCET step: $[Ru^{IV}\{N(H)S^tBu\}(L)(NCCH_3)]^+ + H^+ + e \rightarrow [Ru^{III}\{N(H)_2S^tBu\}(L)(NCCH_3)]^+$, with H^+ presumably coming from H_2O in the solvent. Upon addition of Et_3N (1% by volume), the color of the solution of **2a** changed from blue to orange and

(13) Altomare, A.; Cascarano, G.; Giacovazzo, C.; Guagliardi, A.; Burla, M. C.; Polidori, G.; Camalli, M. *J. Appl. Crystallogr.* **1994**, *27*, 435.
(14) Sheldrick, G. M. *SADABS, Empirical Absorption Correction Program*; University of Gottingen: Gottingen, Germany, **1997**.
(15) *CrystalStructure, Single Crystal Structure Analysis software*, version 3.5.1; Rigaku/MSC Corp.: The Woodlands, TX, **2003**. Watkin, D. J.; Prout, C. K.; Carruthers, J. R.; Betteridge, P. W. *Crystals*; Chemical Crystallography Laboratory: Oxford, U.K., 1996; issue 10.

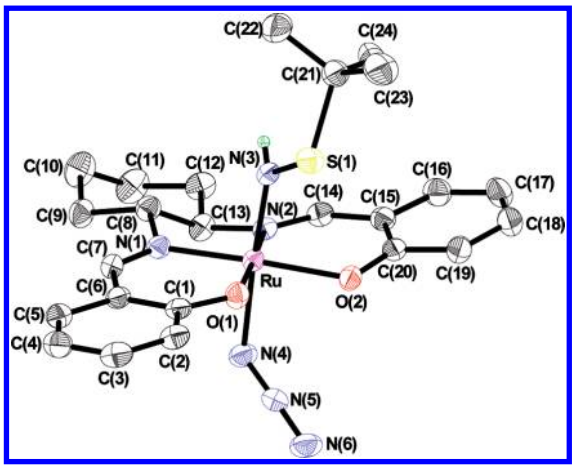

Figure 3. Molecular structure of **2c**. Thermal ellipsoids are drawn at 30% probability. H atoms [except N(3)−H] are omitted for clarity.

the cyclic voltammogram now shows two reversible waves centered at −0.22 and −0.72 V; these are assigned as $[Ru^{V}(NS^{t}Bu)(L)(NCCH_3)]^{+}/[Ru^{IV}(NS^{t}Bu)(L)(NCCH_3)]$ and $[Ru^{IV}(NS^{t}Bu)(L)(NCCH_3)]/\ [Ru^{III}(NS^{t}Bu)(L)(NCCH_3)]^{-}$ couples, respectively. In an independent experiment, an orange solid could be isolated by adding Et_3N to **2a** in CH_3CN. The IR spectrum of the solid reveals the disappearance of ν(N−H) and the intense ν(P−F) band due to PF_6^-, and elemental analysis is consistent with the formula $[Ru^{IV}(NS^{t}Bu)(L)(NCCH_3)]$.[16] The orange solid is diamagnetic and is only sparingly soluble in a common organic solvent. In the ^{1}H NMR spectrum in $(CD_3)_2SO$, the methyl protons of acetonitrile and the *tert*-butyl moiety occur as singlets at δ 2.06 and 0.95, respectively. The N−H resonance at δ 16.41 in **2a** was not observed. The compound decomposes in solution to give a paramagnetic species with a half-life of about 10 min at room temperature.

The cyclic voltammogram of **2b** (Figure S3 in the Supporting Information) shows a reversible couple centered at −0.61 V (vs $Cp_2Fe^{+/0}$), which is assigned to the $[Ru^{III}\{N(H)_2SPh\}(L)(NCCH_3)]^{+}/[Ru^{II}\{N(H)_2SPh\}(L)(NCCH_3)]$ couple. The potential for this couple is 60 mV higher than that of **2a**, in accordance with the PhS substituent being less electron-donating than the ^{t}BuS substituent. There are also a number of irreversible waves, which probably arise from metal-centered $Ru^{IV/III}$, $Ru^{V/IV}$, and ligand-centered oxidations.

The reaction of **2a** with NaN_3 in methanol produced **2c** as sparingly soluble dark-red crystals in high yield. Room temperature magnetic measurement indicates that **2c** is also diamagnetic.[17] In the IR spectrum, the ν(N−H) band shifts from 3236 cm^{-1} in **2a** to 3076 cm^{-1}. The intense ν(P−F) band at 845 cm^{-1} in **2a** disappears, while a strong $\nu(N_3)$ band at 2034 cm^{-1} is observed.

X-ray Structure of $[Ru^{IV}\{N(H)S^{t}Bu\}(L)(N_3)]\cdot CH_3OH$. The X-ray structure of **2c** has been determined (Figure 3). The details of the crystal data are summarized in Tables 1 and 2. Compound **2c** has a distorted octahedral geometry;

Table 2. Selected Bond Distances (Å) and Angles (deg) for **2c**

Bond Distance			
Ru−N(1)	1.995(4)	N(3)−S(1)	1.635(5)
Ru−N(2)	1.991(5)	N(1)−C(7)	1.282(6)
Ru−N(3)	1.902(4)	N(2)−C(14)	1.284(6)
Ru−N(4)	2.101(5)	N(4)−N(5)	1.182(7)
Ru−O(1)	2.014(4)	N(5)−N(6)	1.159(7)
Ru−O(2)	2.030(3)		
Bond Angle			
N(3)−Ru−N(4)	175.7(2)	Ru−N(3)-S(1)	121.6(2)
N(3)−Ru−N(1)	95.5(2)	Ru−N(4)-N(5)	121.3(4)
N(3)−Ru−N(2)	90.3(2)	Ru−N(1)-C(7)	138.49(35)
N(3)−Ru−O(1)	92.1(2)	Ru−N(2)-C(14)	121.24(51)
N(3)−Ru−O(2)	87.8(2)	N(4)−N(5)−N(6)	175.6(7)

the ruthenium center is surrounded by the two O and two N atoms of the salen ligand in the equatorial plane. The axial positions are occupied by one sulfilamido ligand and one azido ligand. This is the first crystal structure of a ruthenium compound bearing a sulfilamido ligand. The Ru−N(sulfilamido) distance of 1.902(4) Å and the acute Ru−N(3)−S(1) angle of 121.6(2)° are comparable to a structurally similar ruthenium(IV) hydrazido(1−) complex $[Ru^{IV}\{N(H)NC_4H_8\}(L)\{N(H)C_4H_8\}]^{+}$,[8] which has a Ru−N(hydrazido) distance of 1.940(5) Å and a Ru−N−N angle of 129.4(4)°. The rather long N(3)−S(1) distance of 1.635(5) Å, and the N(3)−S(1)−C(21) angle of 106.97(27)° are consistent with pseudo-sp^3 hybridization at the S atom. The Ru−N(azido) bond distance of 2.101(5) Å is slightly shorter than that in $[Ru^{II}(tpy)(PPh_3)_2(N_3)](ClO_4)$ [2.132(5) Å].[18]

Reaction of 2a with RSH: Formation of 3. The reaction of **2a** with 1 equiv of RSH (R = ^{t}Bu or Ph) in CH_3CN afforded the green ruthenium(III) sulfilamine species **3** in high yield. By evaporation of the filtrate followed by extraction with Et_2O, 0.45 equiv of RSSR could be isolated (90% yield, characterized by ^{1}H NMR and GC−MS). The reaction is faster with PhSH than with ^{t}BuSH. Compound **3** can also be prepared by the reaction of **1** with 2 equiv of ^{t}BuSH. **3** is paramagnetic with one unpaired electron (μ_{eff} = 1.98 μ_B, Gouy method). The IR spectrum of **3** shows two weak ν(N−H) stretches at 3289 and 3133 cm^{-1}. ESI/MS of **3** in CH_3CN (Figure S2 in the Supporting Information) displays a predominant peak at m/z 568 ($[M]^+$) and a smaller peak at m/z 527 ($[M - CH_3CN]^+$). The cyclic voltammogram of **3** exhibits a reversible $Ru^{III/II}$ couple centered at −0.67 V and an irreversible oxidation wave at +0.65 V vs $Cp_2Fe^{+/0}$ (Figure S4 in the Supporting Information). The reaction of **2a** with RSH may be represented by eq 2.

$$[Ru^{IV}\{N(H)S^{t}Bu\}(L)(NCCH_3)]^{+} + RSH \rightarrow [Ru^{III}\{N(H)_2S^{t}Bu\}(L)(NCCH_3)]^{+} + \frac{1}{2}\,RSSR \quad (2)$$

Reaction of 2b with PhSH: Formation of 4. In contrast to **2a**, the reaction of **2b** with 1 or 2 equiv of PhSH in CH_3CN at room temperature did not produce the corresponding ruthenium(III) sulfilamine species; instead, the

(16) Et_3N (180 mg, 2.0 mmol) was added to a purple solution of **2a** (71 mg, 0.1 mmol) in CH_3CN (2 mL) at room temperature. After 1 h, the orange solid was filtered, washed with CH_3CN (3 × 1 mL), and then air-dried. Yield: 90%. Anal. Calcd (found) for $C_{26}H_{32}N_4O_2SRu$: C, 55.20 (55.15); H, 5.70 (5.89); 9.90 (9.71).

(17) Because of the poor solubility of **2c** in organic solvents, ^{1}H NMR and CV experiments were not carried out.

(18) Seok, W. K.; Yim, S. B.; Klapotke, T. M.; White, P. S. *J. Organomet. Chem.* **1998**, *559*, 165–171.

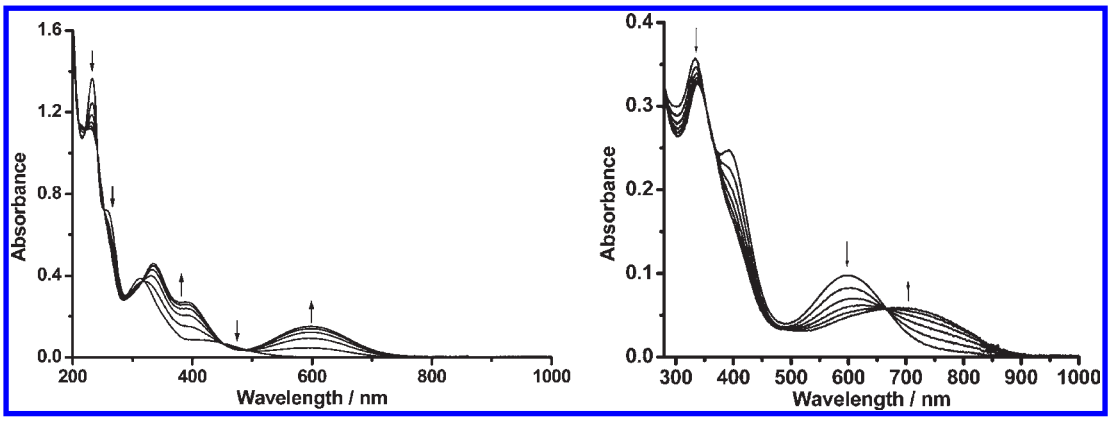

Figure 4. Spectral changes for the reaction of **1** (3.3×10^{-5} M) with ^{t}BuSH in CH_3CN at 298.0 K. The left panel shows the first step (k_a path) at 200 s intervals ([^{t}BuSH] = 3.3×10^{-4} M; total reaction time = 1000 s). The right panel shows the second step (k_b path) at 840 s intervals ([^{t}BuSH] = 1.6×10^{-3} M; total reaction time = 4200 s).

ruthenium(III) ammine compound **4** was isolated, together with 1.35 equiv of PhSSPh (90% yield). Other solvents such as $(CH_3)_2CO$, CH_3OH, or CH_2Cl_2 can also be used. Compound **4** is more conveniently prepared by the direct reaction of **1** with 3 equiv of PhSH. A similar reaction also occurs with 3,5-$Me_2C_6H_3SH$. The reaction of **2b** and **1** with PhSH can be represented by eqs 3 and 4, respectively.

$$[Ru^{IV}\{N(H)SPh\}(L)(NCCH_3)]^+ + 2PhSH \rightarrow [Ru^{III}(NH_3)(L)(NCCH_3)]^+ + \frac{3}{2}PhSSPh \quad (3)$$

$$[Ru^{VI}(N)(L)(NCCH_3)]^+ + 3PhSH \rightarrow [Ru^{III}(NH_3)(L)(NCCH_3)]^+ + \frac{3}{2}PhSSPh \quad (4)$$

Compound **4** has a room temperature magnetic moment of $\mu_{eff} = 2.04\ \mu_B$, which is within the range (1.86−2.07 μ_B) reported for other (salen)ruthenium(III) complexes.[19] The cyclic voltammogram of **4** (Figure S5 in the Supporting Information) shows two reversible waves centered at +0.60 and −0.76 V vs $Cp_2Fe^{+/0}$, which are assigned to $Ru^{IV/III}$ and $Ru^{III/II}$ couples, respectively. Similar reversible couples were also observed in other (salen)ruthenium(III) complexes. For example, $[Ru^{III}(L)(py)_2]^+$ exhibits reversible $Ru^{IV/III}$ and $Ru^{III/II}$ couples at 0.69 and −0.59 V vs $Cp_2Fe^{+/0}$, respectively.[19] ESI/MS (positive mode, CH_3CN) of **4** exhibits a single peak at m/z 480 ($[M]^+$) (Figure S6 in the Supporting Information). The IR spectrum (KBr disk) of **4** shows three sharp ν(N−H) stretches at 3341, 3237, and 3135 cm^{-1}.

X-ray Structure of $[Ru^{III}(NH_3)(L)(NCCH_3)](PF_6)\cdot CH_3CN$. The X-ray structure of **4** has been determined (Figure S7 in the Supporting Information). The crystal data and structure refinement details are given in Table 1. Selected bond distances and angles are listed in Table S1 in the Supporting Information. Compound **4** adopts a distorted octahedral geometry; the Ru−N(salen) [1.973(3) and 1.982(3) Å] and the Ru−O(salen) [2.011(3) and 2.008(3) Å] distances are similar to those in other (salen)ruthenium(III) complexes.[19] The Ru−N(NH_3) distance of 2.083(4) Å is similar to the Ru−N($NCCH_3$) distance of 2.069(3) Å, suggesting that it is a neutral ammine ligand. This Ru−N(NH_3) distance is also comparable to that in $[Ru^{III}(NH_3)_6]^{3+}$ [2.104(4) Å].[20]

Kinetics of the Reaction of 1 with RSH. Figure 4 shows the UV/vis spectral changes that occur when **1** (3.3×10^{-5} M) is mixed with excess ^{t}BuSH (3.3×10^{-4} and 1.6×10^{-3} M) in CH_3CN at 298.0 K under argon. Two well-separated consecutive steps can be observed. Well-defined isosbestic points are maintained at 223, 242, 253, 318, 450, and 489 nm for the first step and at 664 nm for the second step.

The final spectra for the first and second steps are the same as those of **2a** and **3**, respectively. The same spectral changes as those of the second step were also observed when **2a** was mixed with excess ^{t}BuSH. Hence, the reaction scheme is **1** → **2a** → **3**. Analysis of the organic products by GC−MS indicated the formation of 0.5 equiv of ^{t}BuSS^{t}Bu. Hence, the stoichiometry for the two steps can be represented by eqs 1 and 2 (R = ^{t}Bu).

The kinetics of the reaction of **1** with ^{t}BuSH were followed at 600 nm. In the presence of at least 10-fold excess of ^{t}BuSH, clean pseudo-first-order kinetics were observed for both steps for over 3 half-lives (Figure S8 in the Supporting Information). The pseudo-first-order rate constants, k_{obs}, are independent of the concentration of **1** (2.0×10^{-5}−5.0×10^{-5} M) but depend linearly on the concentration of ^{t}BuSH (5.0×10^{-4}−4.0×10^{-1} M; Figure S9 in the Supporting Information) for both steps. Representative data are collected in Table S1 in the Supporting Information. The experimental rate laws for the first and second steps are shown in eqs 5 and 6.

$$-\frac{d[Ru^{VI}(N)]}{dt} = k_a[^tBuSH][Ru^{VI}(N)] \quad (5)$$

$$-\frac{d[Ru^{IV}\{N(H)S^tBu\}]}{dt} = k_b[^tBuSH][Ru^{IV}\{N(H)S^tBu\}] \quad (6)$$

k_a and k_b were found to be $(1.55 \pm 0.01) \times 10^1$ and $(1.93 \pm 0.02) \times 10^{-2}\ M^{-1}\ s^{-1}$, respectively, at 298.0 K.

(19) Man, W. L.; Kwong, H. K.; Lam, W. W. Y.; Xiang, J.; Wong, T. W.; Lam, W. H.; Wong, W. T.; Peng, S. M.; Lau, T. C. *Inorg. Chem.* **2008**, *47*, 5936–5944.

(20) Stynes, H. C.; Ibers, J. A. *Inorg. Chem.* **1971**, *10*, 2304–2308.

The effects of the temperature on the rate constants were studied from 288.0 to 318.0 K in CH_3CN. $\Delta H^{\ddagger}$ and $\Delta S^{\ddagger}$ were found to be (10.7 ± 0.3) kcal mol^{-1} and $-(17 \pm 1)$ cal mol^{-1} K^{-1}, respectively, for the k_a path and (19.4 ± 0.4) kcal mol^{-1} and $-(1 \pm 1)$ cal mol^{-1} K^{-1}, respectively, for the k_b path (Figure S10 in the Supporting Information).

The kinetics were also carried out with ^{t}BuSD in CH_3CN at 298.0 K. The second-order rate constants, k_a^D and k_b^D, were found to be $(1.18 \pm 0.02) \times 10^1$ and $(5.96 \pm 0.03) \times 10^{-3}$ M^{-1} s^{-1}, respectively (Table S2 in the Supporting Information). Hence, the kinetic isotope effect (KIE) values for the k_a and k_b (Figure S11 in the Supporting Information) paths are $k_a/k_a^D = 1.3 \pm 0.1$ and $k_b/k_b^D = 3.2 \pm 0.1$, respectively.

The reaction of **1** with PhSH (1.0×10^{-2}–2.0×10^{-1} M) has also been investigated in CH_3CN at 298.0 K. Two steps were also observed; the final spectra for the first and second steps are the same as those of **2b** and **4**, respectively. The same spectral changes as those of the second step were also observed when **2b** was mixed with excess PhSH. Hence, the reaction scheme is **1** → **2b** → **4**, and the two steps can be represented by eqs 1 and 3 (R = Ph). The second-order rate constants for the first and second steps, k_a' and k_b', are $(1.38 \pm 0.03) \times 10^3$ and $(3.10 \pm 0.14) \times 10^1$ M^{-1} s^{-1}, respectively. $\Delta H^{\ddagger}$ and $\Delta S^{\ddagger}$ are (11.8 ± 0.5) kcal mol^{-1} and $-(5 \pm 1)$ cal mol^{-1} K^{-1}, respectively, for the k_a path and (13.6 ± 0.8) kcal mol^{-1} and $-(6 \pm 1)$ cal mol^{-1} K^{-1}, respectively, for the k_b path (Figure S12 in the Supporting Information). The kinetics of oxidation of PhSD (>95% D) by **1** were also studied in CH_3CN at 298.0 K; the KIE values for the k_a' and k_b' steps are found to be 1.0 ± 0.1 and 2.6 ± 0.2, respectively (Figure S13 in the Supporting Information). Similar kinetic behaviors were observed when 3,5-$Me_2C_6H_3SH$ was used as the substrate; k_a'' and k_b'' are $(2.53 \pm 0.05) \times 10^3$ and $(2.50 \pm 0.01) \times 10^1$ M^{-1} s^{-1}, respectively (Table S2 in the Supporting Information).

C−H Bond Activation by [Ru^{IV}{N(H)SR}(L)(NCCH$_3$)]$^+$. Compounds **2a** and **2b** react readily with hydrocarbons containing weak C−H bonds. The UV/vis spectral changes that occurred when [Ru^{IV}{N(H)S^{t}Bu}(L)(NCCH$_3$)]$^+$ was mixed with an excess of DHA in CH_3CN at 298.0 K are shown in Figure 5. The appearance of a peak at 685 nm indicates the formation of **3**. The conversion of **2a** to **3** can also be monitored by ESI/MS, which shows that the peak at m/z 567 ([M]$^+$) for **2a** is shifted to 568 upon the addition of DHA (Figure S14 in the Supporting Information). Analysis of the organic products by GC−MS showed that 0.4 equiv of anthracene was produced (80% yield; eq 7).

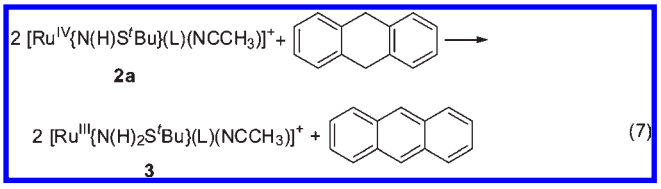

(7)

In the presence of at least 10-fold excess of DHA, the decay of **2a** monitored at 600 nm follows clean pseudo-first-order kinetics for over 3 half-lives. The pseudo-first-order rate constant, k_{obs}, is independent of the concentration of Ru^{IV} (3×10^{-5}–1×10^{-4} M) but depends linearly on the concentration of DHA (1×10^{-2}–1×10^{-1} M)

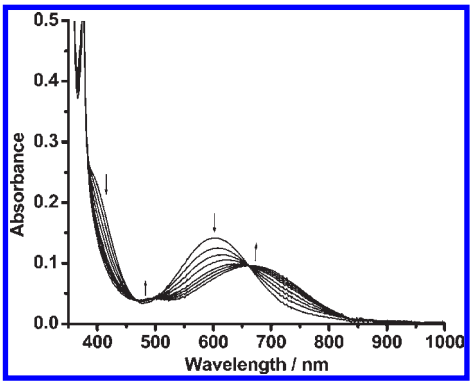

Figure 5. Spectrophotometric changes at 1200 s intervals for the reduction of **2a** (4.0×10^{-5} M) by DHA (3.1×10^{-2} M) at 298.0 K in CH_3CN.

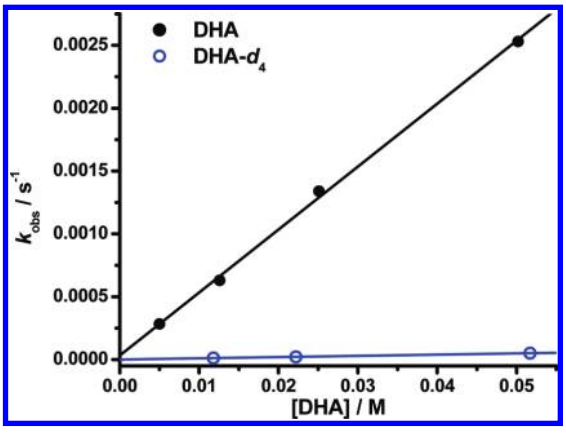

Figure 6. Plot of k_{obs} vs [DHA] (solid circle) and [DHA-d_4] (open circle) for the reaction of DHA with **2a** (3.65×10^{-5} M) in CH_3CN at 298.0 K. [For DHA: slope = $(5.01 \pm 0.23) \times 10^{-2}$; y intercept = $(3.26 \pm 7.70) \times 10^{-5}$; r = 0.9989. For DHA-d_4: slope = $(9.77 \pm 0.25) \times 10^{-4}$; y intercept = $(5.16 \pm 8.81) \times 10^{-7}$; r = 0.9996.]

(Figure 6). Kinetic data are collected in Table 3. At 298 K, the second-order rate constant $k_2 = (5.01 \pm 0.23) \times 10^{-2}$ M^{-1} s^{-1}. The activation parameters, $\Delta H^{\ddagger}$ and $\Delta S^{\ddagger}$, determined by studying the kinetics over a 30 °C temperature range, are (13.8 ± 0.4) kcal mol^{-1} and $-(18 \pm 4)$ cal mol^{-1} K^{-1}, respectively (Figure S15 in the Supporting Information). DHA-d_4 (deuterated at aliphatic C−H bonds) reacts with **2a** at a substantially slower rate than DHA, k_2(DHA-d_4) = $(9.77 \pm 0.25) \times 10^{-4}$ M^{-1} s^{-1}. KIE, k_2(DHA)/k_2(DHA-d_4), is 51 ± 1 at 298.0 K in CH_3CN.[21]

2a also reacts with CHD to give **3** and 0.4 equiv of benzene (80% yield), k_2(CHD) at 298 K = 6.83×10^{-2} M^{-1} s^{-1}. KIE = k_2(CHD)/k_2(CHD-d_8) = 56 ± 2 at 298 K (Figure S16 in the Supporting Information).[21] The kinetics of the reaction of **2a** with xanthene, fluorene, diphenylmethane, and triphenylmethane have also been studied, and the data are collected in Table 3.[22] The second-order rate constants are listed as k'_2, which is equal to k_2 divided by the number of reactive H atoms in

(21) These are minimum values of the true KIE because the substrates are "> 99%" but not 100% enriched.

(22) No coupling or other products was detected by GC−MS for these substrates. Small amounts of ^{t}BuS^{t}Bu, (^{t}BuS)$_2$, and ^{t}BuSSS^{t}Bu were detected. However, ESI/MS of a reaction mixture of **2a** (0.01 M) with Ph_2CH_2 (1.0 M) in CH_3CN (1 mL) shows a peak at m/z 605, which is assigned to [Ru{N(H)$_2$CHPh$_2$}(L)(NCCH$_3$)]$^+$ (Figure S17 in the Supporting Information). Presumably, for these substrates, at least some of the carbon radicals produced from HAT were combined with the metal complex.

Table 3. Representative Data for the Reaction of Hydrocarbons with **2a** (3.15×10^{-5} M) in CH_3CN at 298.0 K

substrate	T/K	k'_2[a]/M^{-1} s^{-1}	BDEs/kcal mol^{-1}
xanthene	298.0	$(2.39 \pm 0.10) \times 10^{-2}$	75.5[23]
CHD	298.0	$(1.71 \pm 0.07) \times 10^{-2}$	77.0[24]
		$(3.08 \pm 0.25) \times 10^{-4}$ [b]	
DHA	298.0	$(1.25 \pm 0.12) \times 10^{-2}$	78.0[23]
		$(2.44 \pm 0.06) \times 10^{-4}$ [c]	
	288.0	$(5.69 \pm 0.27) \times 10^{-3}$	
	308.0	$(2.72 \pm 0.09) \times 10^{-2}$	
	318.0	$(6.21 \pm 0.49) \times 10^{-2}$	
	298.0	$(3.08 \pm 0.18) \times 10^{-3}$ [d]	
		$(1.05 \pm 0.03) \times 10^{-4}$ [c,d]	
fluorene	298.0	$(8.82 \pm 0.51) \times 10^{-3}$	80.1[23]
		$(8.10 \pm 0.35) \times 10^{-4}$ [e]	
triphenylmethane	298.0	$(1.51 \pm 0.08) \times 10^{-4}$	81.0[23]
diphenylmethane	298.0	$(2.80 \pm 0.13) \times 10^{-4}$	82.0[23]
	291.2	$(1.28 \pm 0.07) \times 10^{-4}$	
	308.5	$(9.15 \pm 0.93) \times 10^{-4}$	
	317.5	$(2.74 \pm 0.16) \times 10^{-3}$	

[a] k_2' is equal to k_2 divided by the number of active H atoms. [b] CHD-d_8 was used. [c] DHA-d_4 was used. [d] **2b** (3.90×10^{-5} M) was used. [e] Fluorene-d_{10} was used.

each substrate. For example, the number of reactive H atoms for xanthene and DHA are 2 and 4, respectively. $\Delta H^{\ddagger}$ and $\Delta S^{\ddagger}$ for the reaction with diphenylmethane were found to be (20.7 ± 0.6) kcal mol^{-1} and −(4 ± 1) cal mol^{-1} K^{-1}, respectively (Figure S18 in the Supporting Information). The KIE value for the oxidation of fluorene by Ru^{IV}, k_2(fluorene)/k_2(fluorene-d_{10}) is (11 ± 1) at 298.0 K (Figure S19 in the Supporting Information).

The kinetics for the reaction of DHA with **2b** were also studied. In the presence of at least a 10-fold excess of DHA in CH_3CN, clean pseudo-first-order kinetics were observed for over 3 half-lives. The pseudo-first-order rate constant, k_{obs}, is independent of the concentration of Ru^{IV} but depends linearly on the concentration of DHA (0.01−0.04 M). The second-order rate constant k_2 = $(1.23 \pm 0.07) \times 10^{-2}$ M^{-1} s^{-1} at 298 K, which is about 4 times slower than the reaction with **2a** (Figure S20 in the Supporting Information). KIE, k_2(DHA)/k_2(DHA-d_4), is (29 ± 2) at 298.0 K.[21] Analysis of the organic products by GC−MS indicated the formation of 0.7 mol equiv of anthracene and 0.3 mol equiv of PhSSPh; the yields are 70% and 60%, respectively, according to eq 8. ESI/MS of the solution after reaction shows a predominant peak at m/z 480, which is due to $[Ru(NH_3)(L)(NCCH_3)]^+$ (Figure S21 in the Supporting Information). There are also minor peaks at m/z 504, 531, and 658; which may be tentatively assigned to $[Ru(L)(NCCH_3)_2]^+$, $[Ru(SPh)(L)]^+$, and $[Ru\{N(H)C_{14}H_{10}\}(L)(NCCH_3)]^+$, respectively. These may account for some of the "missing" anthracene and PhSSPh not detectable by GC−MS (eq 8).

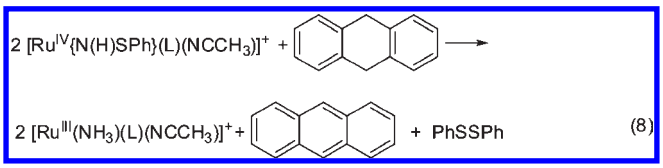

Discussion

The electrophilic (salen)ruthenium(VI) nitrido species **1** undergoes stepwise reactions with RSH to produce

Scheme 1. Reaction of **1** with RSH

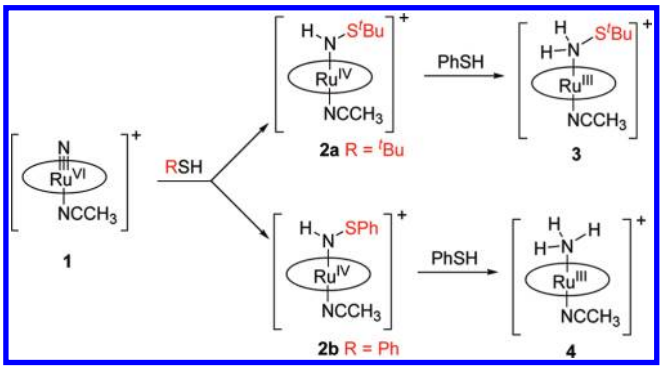

ruthenium(IV) sulfilamido, ruthenium(III) sufilamine, or ruthenium(III) ammine species, depending on the nature of R and the number of equivalents of RSH used (Scheme 1).

Mechanism of the Formation of Ruthenium(IV) Sulfilamido Species. The reaction of **1** with 1 equiv of RSH produces $[Ru^{IV}\{N(H)SR\}(L)(NCCH_3)]PF_6$ (**2a**, R = ^{t}Bu; **2b**, R = Ph). A similar reaction occurs between *cis*- or *trans*-$[Os^{VI}(tpy)(N)(Cl)_2]^+$ and 3,5-$Me_2C_6H_3SH$ to produce *cis*- or *trans*-osmium(IV) sulfilimido species $[Os^{IV}(tpy)\{NS(H)C_6H_3Me_2\}Cl_2]$.[4] In the osmium case, the S atom is protonated rather than the N atom, with the ν(S−H) stretch occurring at 1944 and 2249 cm^{-1}, respectively, for the cis and trans isomers. No ν(S−H) stretch can be found in the IR spectra of **2a** or **2b**.

The observed second-order rate law and the small deuterium isotope effects suggest that the formation of ruthenium(IV) sulfilamido species occurs via a rate-limiting nucleophilic attack of RSH at Ru^{VI}≡N followed by a proton shift. The less electron-rich aromatic thiols react faster than ^{t}BuSH by 2 orders of magnitude, probably because of larger steric effects of the *tert*-butyl group. The more negative $\Delta S^{\ddagger}$ for the reaction of **1** with ^{t}BuSH ($\Delta H^{\ddagger}$ = 10.7 ± 0.3 kcal mol^{-1}; $\Delta S^{\ddagger}$ = −17 ± 1 cal mol K^{-1}) than with PhSH ($\Delta H^{\ddagger}$ = 11.8 ± 0.5 kcal mol^{-1}; $\Delta S^{\ddagger}$ = −5 ± 1 cal mol K^{-1}) reflects a more ordered transition state for the former reaction that is imposed by the more bulky *tert*-butyl group. **1** is 2 and 4 orders of magnitude more reactive than *cis*- and *trans*-$[Os^{VI}(N)(tpy)Cl_2]^+$ (k = 3.21 ± 0.06 M^{-1} s^{-1} and (3.60 ± 0.08) × 10^{-2} M^{-1} s^{-1}), respectively, in the reaction with 3,5-$Me_2C_6H_3SH$,[4] which is as expected because high-valent ruthenium complexes are, in general, more electrophilic/oxidizing than the corresponding osmium complexes.[25]

Mechanism of the Formation of Ruthenium(III) Sulfilamine and Ruthenium(III) Ammine Species. 2a reacts with 1 equiv of RSH to produce **3** and 0.5 equiv of RSSR according to eq 2. The observed formation of RSSR and the deuterium isotope effect of 3.2 are consistent with a mechanism involving rate-limiting H-atom

(23) Gardner, K. A.; Kuehnert, L. L.; Mayer, J. M. *Inorg. Chem.* **1997**, *36*, 2069–2078.
(24) Laarhoven, L. J. J.; Mulder, P.; Wayner, D. D. M. *Acc. Chem. Res.* **1999**, *32*, 342–349.
(25) Che, C. M.; Lau, T. C. In *Comprehensive Coordination Chemistry II*; McCleverty, J. A., Meyer, T. J., Eds.; Elsevier: Oxford, U.K., 2003; pp 733−847.

Scheme 2. Proposed Mechanism for the Formation of $[Ru^{III}(NH_3)(L)(NCCH_3)]^+$

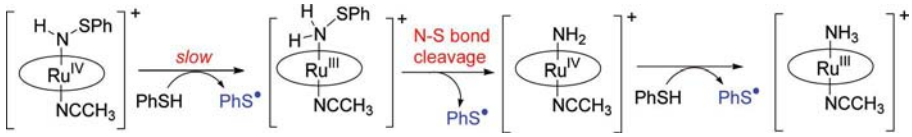

abstraction (HAT) from RSH by $[Ru^{IV}\{N(H)S^tBu\}(L)(NCCH_3)]^+$.[26] The aromatic thiols (PhSH and 3,5-$Me_2C_6H_4SH$) react faster than ^{t}BuSH by 3 orders of magnitude, which is likely due to a lower S−H bond dissociation energy (BDE) of the aromatic thiols (S−H BDE for PhSH and ^{t}BuSH are 79.1 and 88.6 kcal mol^{-1}, respectively).[27,28] This is also reflected by a lower $\Delta H^{\ddagger}$ for the reaction with PhSH ($\Delta H^{\ddagger} = 13.6 \pm 0.8$ kcal mol^{-1}; $\Delta S^{\ddagger} = -6 \pm 1$ cal mol K^{-1}) than with ^{t}BuSH ($\Delta H^{\ddagger} = 19.4 \pm 0.4$ kcal mol^{-1}; $\Delta S^{\ddagger} = -1 \pm 1$ cal mol K^{-1})

2b also reacts with PhSH, but the product is the ruthenium(III) ammine complex **4** irrespective of the number of equivalents of PhSH used. A total of 1.5 equiv of PhSSPh is produced when 2 equiv or more of PhSH is used. No intermediate ruthenium sulfilamine species $[Ru^{III}\{N(H)_2SPh\}(L)(NCCH_3)]^+$ could be isolated or detected by ESI/MS. This reaction occurs with a deuterium isotope effect of 2.6, suggesting that the rate-limiting step also involves HAT. A proposed mechanism is shown in Scheme 2.

The initial rate-limiting step involves HAT from PhSH by ruthenium(IV) to generate $[Ru^{III}\{N(H)_2SPh\}(L)(NCCH_3)]^+$ and PhS$^{\bullet}$, which undergoes rapid N−S cleavage to produce a ruthenium(IV) amido species $[Ru^{IV}(NH_2)(L)(NCCH_3)]^+$ and PhS$^{\bullet}$. $[Ru^{IV}(NH_2)(L)(NCCH_3)]^+$ then abstracts a H atom from another molecule of PhSH to give the ruthenium(III) ammine product and PhS$^{\bullet}$.[29]

Compound **4** can be prepared directly from the reaction of **1** with 3 equiv of PhSH; the overall reaction (eq 4) represents the reduction of $Ru^{VI}{\equiv}N$ to $Ru^{III}-NH_3$ by PhSH. The reduction of a metal nitrido species to the ammine is a key process in biological and chemical nitrogen fixation.[30−37] This reduction process is usually carried out by using a combination of a proton source and a reducing agent. For example, $[Os^{VI}(N)Cl_3(py)_2]$ and $[Os^{VI}(Tp)(N)Cl_2]$ are reduced by $SnCl_2 \cdot H_2O$ in HCl/CH_3OH to $[Os^{III}(NH_3)Cl_3(py)_2]$ and $[Os^{III}(Tp)(NH_3)Cl_2]$, respectively.[38−40] $[Os^{VI}(tpy)(N)Cl_2]$ and $[Os^{VI}(tpm)(N)Cl_2]$ can be reduced to the corresponding osmium(III) ammines by hydrochloric acid and zinc amalgam.[39,40] In the catalytic reduction of dinitrogen to ammonia by molybdenum catalysts bearing tetradentate triamidoamine ligands, a 2,6-lutidinium salt and decamethylchromocene are used to reduce the intermediate molybdenum nitrido species.[35]

Mechanism of C−H Bond Activation by $[Ru^{IV}\{N(H)SR\}(L)(NCCH_3)]^+$. The observed ability of **2a** and **2b** to abstract H atoms from thiols such as ^{t}BuSH (BDE = 88.6 kcal mol^{-1})[27] or PhSH (BDE = 79.1 kcal mol^{-1})[28] suggests that they may also be able to abstract H atoms from hydrocarbons with weak C−H bonds. Indeed, **2a** readily reacts with DHA to give **3** and anthracene with a KIE value of 51. Large KIE values are also observed for CHD and fluorene, which implies C−H cleavage in the rate-limiting step.[26] Two possible mechanisms that are consistent with the observed kinetic results are initial rate-limiting HAT from RH by **2a** and initial rate-limiting proton transfer from RH to **2a**, followed by fast electron transfer. The latter mechanism has been found for the dehydrogenation of alkylaromatics by a strongly basic amidoruthenium complex *trans*-$[(DMPE)_2Ru(H)(NH_2)]$.[41] In the present case, the kinetic data are more consistent with a HAT mechanism. For example, fluorene has a much lower pK_a (22.6) than xanthene (30.0), yet it reacts 3 times slower with **2a**, which is inconsistent with a proton-transfer mechanism. On the other hand, fluorene has a larger C−H BDE (80.1 kcal mol^{-1}) than xanthene (75.5 kcal mol^{-1}); hence, it should react more slowly than xanthene if the mechanism is HAT. Mayer and co-workers have shown that, for a number of HAT reactions, a linear correlation occurs between log(rate constant) and BDE.[23,26,42−44] In this case, a plot of log k'_2 vs C−H BDE of the hydrocarbons (Figure 7) shows a good linear relationship for xanthene, CHD, DHA, and fluorene. However, the more bulky diphenylmethane and triphenylmethane react much more slowly than expected from their BDEs; simple molecular modeling shows that there is substantial steric hindrance for HAT by **2a** and **2b** from these substrates. The larger $\Delta S^{\ddagger}$ for diphenylmethane ($\Delta H^{\ddagger} = 20.7 \pm 0.6$ kcal mol^{-1};

(26) KIE for HAT can range from 2 to 450. For example, see:(a) Mayer, J. M. *Acc. Chem. Res.* **1998**, *31*, 441–450. (b) Mayer, J. M. *Annu. Rev. Phys. Chem.* **2004**, *55*, 363–390. (c) Huynh, M. H. V.; Meyer, T. J. *Proc. Natl. Acad. Sci. U.S.A.* **2004**, *101*, 13138–13141.

(27) Luo, Y. R. *Handbook of Bond Dissociation Energies in Organic Compounds*; CRC Press: New York, 2003.

(28) Bordwell, F. G.; Zhang, X. M.; Satish, A. V.; Cheng, J. P. *J. Am. Chem. Soc.* **1994**, *116*, 6605–6610.

(29) We thank a reviewer for suggesting an alternative mechanism that involves the direct attack of PhS$^{\bullet}$ on S of $Ru^{III}N(H)_2SPh$ to give PhSSPh and $Ru^{IV}NH_2$. However, we favor the homolysis mechanism because we were not able to generate $[Ru^{III}\{N(H)_2SPh\}(L)(NCCH_3)]^+$ by other means such as treatment with DHA or by electrochemistry, suggesting that the species is unstable.

(30) Fryzuk, M. D.; Kozak, C. M.; Bowdridge, M. R.; Patrick, B. O.; Rettig, S. J. *J. Am. Chem. Soc.* **2002**, *124*, 8389–8397.

(31) Caselli, A.; Solari, E.; Scopelliti, R.; Floriani, C.; Re, N.; Rizzoli, C.; Chiesi-Villa, A. *J. Am. Chem. Soc.* **2000**, *122*, 3652–3670.

(32) Tuczek, F.; Lehnert, N. *Angew. Chem., Int. Ed.* **1998**, *37*, 2636–2638.

(33) Betley, T. A.; Peters, J. C. *J. Am. Chem. Soc.* **2004**, *126*, 6252–6254.

(34) Howard, J. B.; Rees, D. C. *Chem. Rev.* **1996**, *96*, 2965–2982.

(35) Yandulov, D. V.; Schrock, R. R. *Science* **2003**, *301*, 76–78.

(36) Ritleng, V.; Yandulov, D. V.; Weare, W. W.; Schrock, R. R.; Hock, A. S.; Davis, W. M. *J. Am. Chem. Soc.* **2004**, *126*, 6150–6163.

(37) Yandulov, D. V.; Schrock, R. R. *Inorg. Chem.* **2005**, *44*, 1103–1117.

(38) Ware, D. C.; Taube, H. *Inorg. Chem.* **1991**, *30*, 4598–4605.

(39) Coia, G. M.; Demadis, K. D.; Meyer, T. J. *Inorg. Chem.* **2000**, *39*, 2212–2223.

(40) El-Samanody, E. S.; Demadis, K. D.; Meyer, T. J.; White, P. S. *Inorg. Chem.* **2001**, *40*, 3677–3686.

(41) Fulton, J. R.; Sklenak, S.; Bouwkamp, M. W.; Bergman, R. G. *J. Am. Chem. Soc.* **2002**, *124*, 4722–4737.

(42) Bryant, J. R.; Mayer, J. M. *J. Am. Chem. Soc.* **2003**, *125*, 10351–10361.

(43) Cook, G. K.; Mayer, J. M. *J. Am. Chem. Soc.* **1995**, *117*, 7139–7156.

(44) Matsuo, T.; Mayer, J. M. *Inorg. Chem.* **2005**, *44*, 2150–2158.

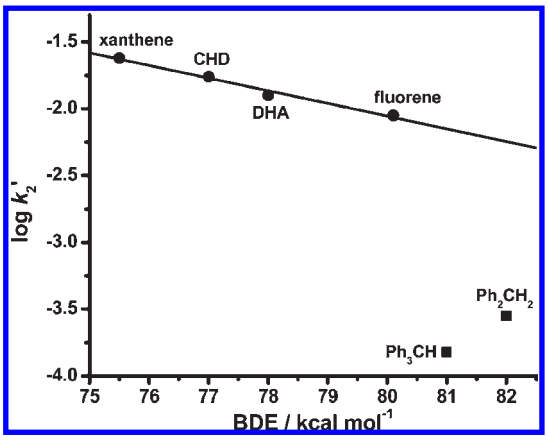

Figure 7. Plot of log k'_2 vs C−H BDEs for the reaction of hydrocarbons with **2a** in CH_3CN at 298.0 K [slope = $-(9.49 \pm 0.84) \times 10^{-2}$; *y* intercept = 5.54 ± 0.66; $r = -0.9922$].

$\Delta S^{\ddagger} = -4 \pm 1$ cal mol^{-1} K^{-1}) than for DHA ($\Delta H^{\ddagger} = 13.8 \pm 0.4$ kcal mol^{-1}; $\Delta S^{\ddagger} = -18 \pm 4$ cal mol^{-1} K^{-1}) may be interpreted as arising from a larger reorganization of ruthenium(IV) in the reaction with diphenylmethane to give a more open structure in the transition state for HAT. Steric effects in HAT have also been observed in the oxidation of phenols[45] and hydroquinones[46] by ruthenium oxo complexes. Although a linear correlation between log(rate constant) and BDE is observed, the slope of the linear plot is −0.09, which is much smaller than the theoretical slope of −0.36 (for small $\Delta G°$) predicted by the Marcus cross relation.[47,48] This seems to argue against a HAT mechanism. However, the range of BDE of the substrates in the linear plot is < 5 kcal. Moreover, BDE for $[Ru^{III}\{N(H)_2S^tBu\}(L)(NCCH_3)]^+$ cannot be determined because of irreversible CV of $[Ru^{IV}\{N(H)S^tBu\}(L)(NCCH_3)]^+$; hence, $\Delta G°$ for HAT is not known. We are currently investigating HAT reactions of more reactive and less hindered ruthenium(IV) amido complexes so that substrates with a wider range of BDE can be investigated without complications from steric effects.

Concluding Remarks

The electrophilic (salen)ruthenium(VI) nitrido species **1** undergoes stepwise reactions with RSH to produce the first examples of sulfilamido and sulfilamine complexes of ruthenium. The direct reduction of **1** to $[Ru^{III}(NH_3)(L)(CH_3CN)]^+$ with PhSH also represents a new method for the conversion of a nitrido species to an ammine. The ruthenium(IV) sulfilamido species, generated from the addition of 1 equiv of RSH to **1**, is able to abstract H atoms from hydrocarbons containing weak C−H bonds. Our preliminary results show that similar ruthenium(IV) species, generated from the addition of 1 equiv of various other nucleophiles such as PPh_3 or 2,3-dimethyl-2-butene,[9] are also able to abstract H atoms from hydrocarbons. Thus, a new class of C−H bond-activating reagents can be readily obtained by the treatment of $Ru^{VI}{\equiv}N$ with a suitable nucleophile.

Acknowledgment. We thank Prof. J. M. Mayer for helpful discussions. We also thank the reviewers for critical comments. The work described in this paper was financially supported by the Research Grants Council of Hong Kong (Grants CityU 101505 and HKU1/CRF/08).

Supporting Information Available: Crystallographic files for **2c** and **4** in CIF format, ^{1}H NMR, CV, ESI/MS, and kinetic data. This material is available free of charge via the Internet at http://pubs.acs.org.

(45) Yiu, D. T. Y.; Lee, M. F. W.; Lam, W. W. Y.; Lau, T. C. *Inorg. Chem.* **2003**, *42*, 1225–1232.

(46) Lam, W. W. Y.; Lee, M. F. W.; Lau, T. C. *Inorg. Chem.* **2006**, *45*, 315–321.

(47) Mayer and co-workers have shown that the Marcus cross relation ($k_{XY} = \sqrt{k_{XX}k_{YY}K_{XY}f_{XY}}$) holds fairly well for a range of PCET/HAT reactions. Using $\Delta G° \approx$ BDE(RH) − BDE($[Ru^{III}\{N(H)_2S^tBu\}(L)(NCCH_3)]^+$) = $-RT$ ln K_{XY}, the plot of log k_{XY} vs BDE(RH) (in kcal mol^{-1}) should have a theoretical slope of −0.36 (k_{XY} = rate constant for the reaction between X and Y; k_{XX} and k_{YY} = self-exchange rate constants for X and Y, respectively; K_{XY} = equilibrium constant for the reaction; f_{XY} = frequency factor).

(48) (a) Roth, J. P.; Yoder, J. C.; Won, T. J.; Mayer, J. M. *Science* **2001**, *294*, 2524–2526. (b) Marcus, R. A.; Eyring, H. *Annu. Rev. Phys. Chem.* **1964**, *15*, 155–196.